Supplementary Information

Cutaneous immuno-surveillance and regulation of inflammation by group 2 innate lymphoid cells

Ben Roediger, Ryan Kyle, Kwok Ho Yip, Nital Sumaria, Thomas V. Guy, Brian S. Kim, Andrew J. Mitchell, Szun S. Tay, Rohit Jain, Elizabeth Forbes-Blom, Xi Chen, Philip L. Tong, Holly A. Bolton, David Artis, William E. Paul, Barbara Fazekas de St. Groth, Michele A. Grimbaldeston, Graham Le Gros & Wolfgang Weninger

Supplementary Figure 1

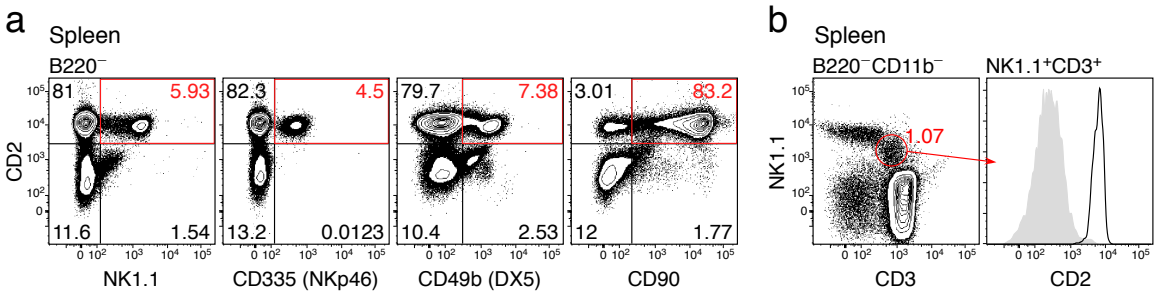

Supplementary Figure 1. CD2 expression by natural killer (NK) and NKT cells. (**a**) Representative dotplots depicting CD2 expression by NK1.1$^+$, NKp46$^+$, DX5$^+$ and CD90$^+$ NK cells in wild-type C57BL/6 mice. (**b**) CD2 expression by splenic CD3$^+$ NK1.1$^+$ NKT cells. Results are representative of 2 independent experiments (n = 4).

Supplementary Figure 2

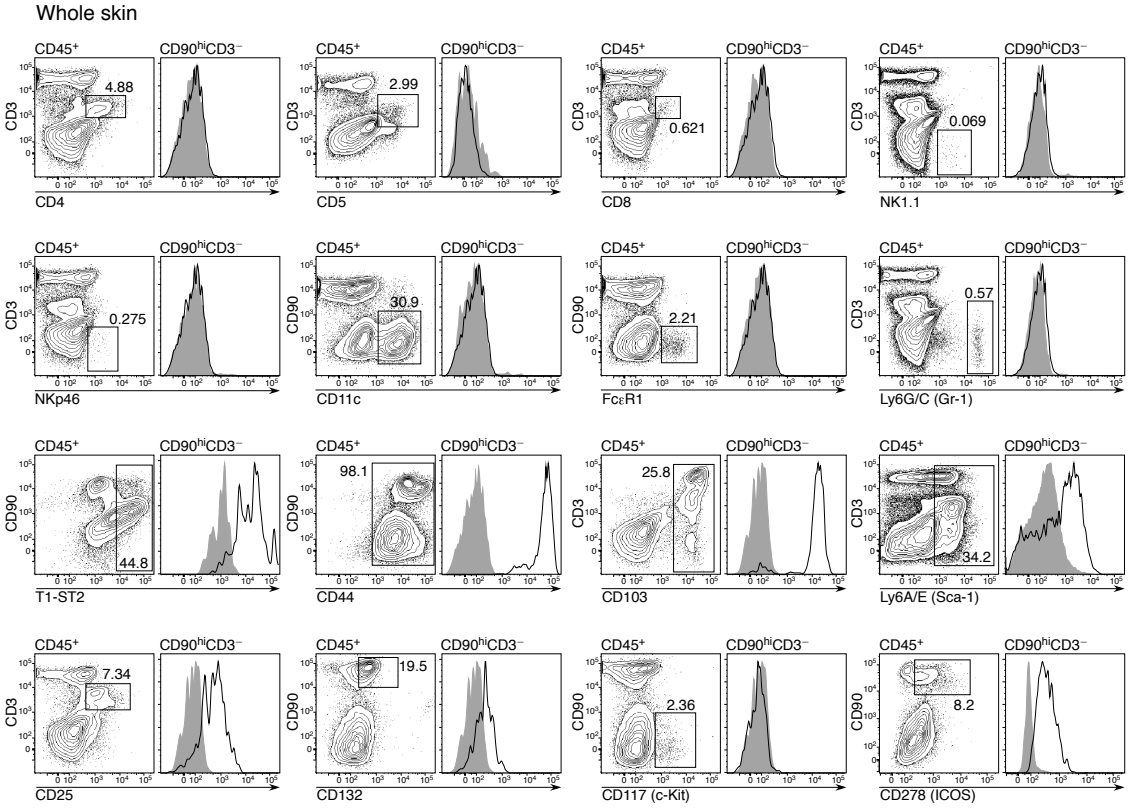

Supplementary Figure 2. Phenotype of skin ILC2. Representative histograms depicting surface expression of indicated markers by $CD45^{+}CD90^{hi}CD3^{-}$ dILC2 isolated from the skin of wild-type mice. Contour plots indicate the presence of other leukocytes bearing the marker of interest within the same sample, a requisite internal positive control to exclude possible misinterpretation due to enzyme cleavage artifacts. Results are compiled from 6 independent experiments ($n \geq 2$ per marker).

Supplementary Figure 3

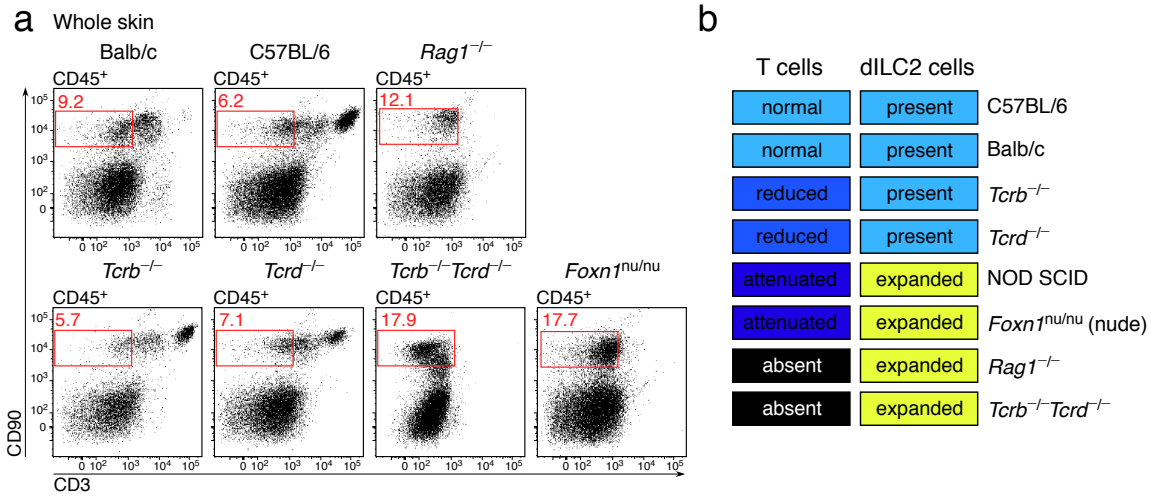

Supplementary Figure 3. Relationship between T cells and ILC in the skin. (**a**) Representative dotplots of $CD45^+$ cells in the skin of indicated mouse strains. Gates indicate $CD90^{hi}$ $CD3^-$ ILCs. Numbers indicate percent positive cells within each gate. (**b**) Summary of T cell and ILC composition in indicated mouse strains. Data are representative of at least two independent experiments for each strain.

Supplementary Figure 4

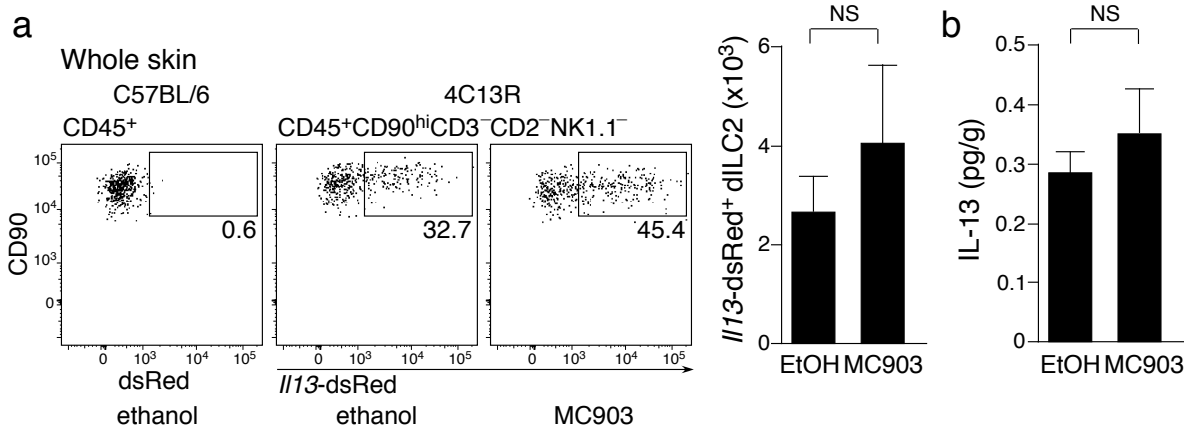

Supplementary Figure 4. IL-13 production by dILC2 in response to MC903 *in vivo*. (**a**) Left, representative dotplots of dILC2 in 4C13R transgenic mice topically treated with MC903 or vehicle (ethanol, EtOH). Right, absolute number of *Il13*-dsRed^{+} dILC2 in 4C13R mice topically treated with MC903 or EtOH. Data are mean ± s.d. and were pooled from 2 independent experiments (n = 6 for MC903, n = 4 for EtOH) (**b**) IL-13 protein detection within skin homogenates of MC903-treated mice and vehicle (ethanol, EtOH) treated controls, as detected by cytokine bead array. Data are mean ± s.d. (n = 5 for MC903, n = 4 for EtOH). NS, not significant.

Supplementary Figure 5

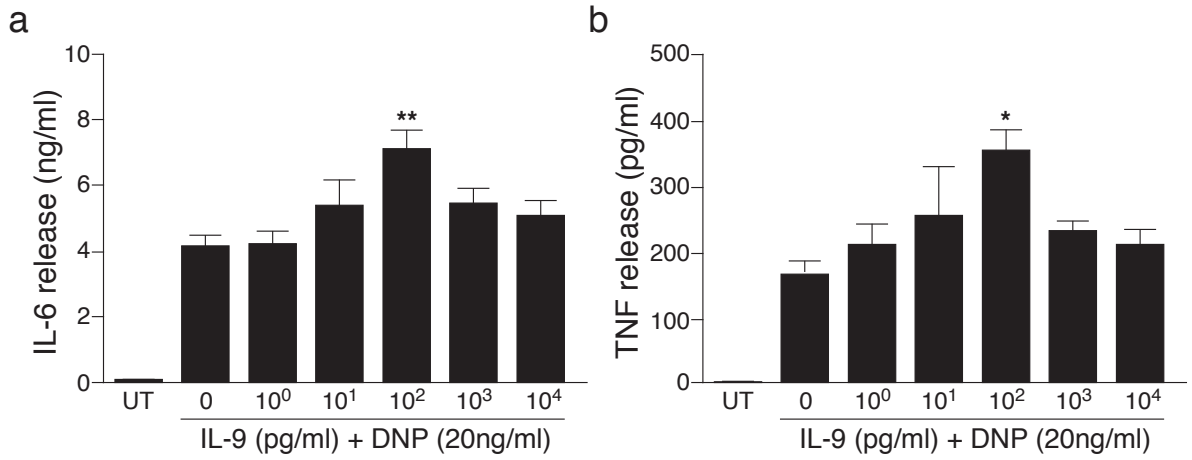

Supplementary Figure 5. Role of ILC2-derived cytokines on mast cell function. (**a**,**b**) Effect of exogenous IL-9 on cytokine production by mast cells *in vitro*. Mast cells were pre-incubated with rmIL-9 (0 – 10,000 pg/ml) and sensitized with anti-DNP IgE (2 μg/ml) for 16 h. Cells were washed and then stimulated with DNP-HSA (20ng/ml) in the presence of rmIL-9 (0 – 10,000 pg/ml) for 6 h. (**a**) IL-6 and (**b**) TNF in supernatant were measured by ELISA. Data in (a) and (b) are expressed as mean ± s.e.m. from 3 independent experiments. Significant differences in cytokine release by DNP alone and in the presence of IL-9 were determined by one way ANOVA with Dunnett's post-test. *$P < 0.05$, ** $P < 0.01$.

Supplementary Figure 6

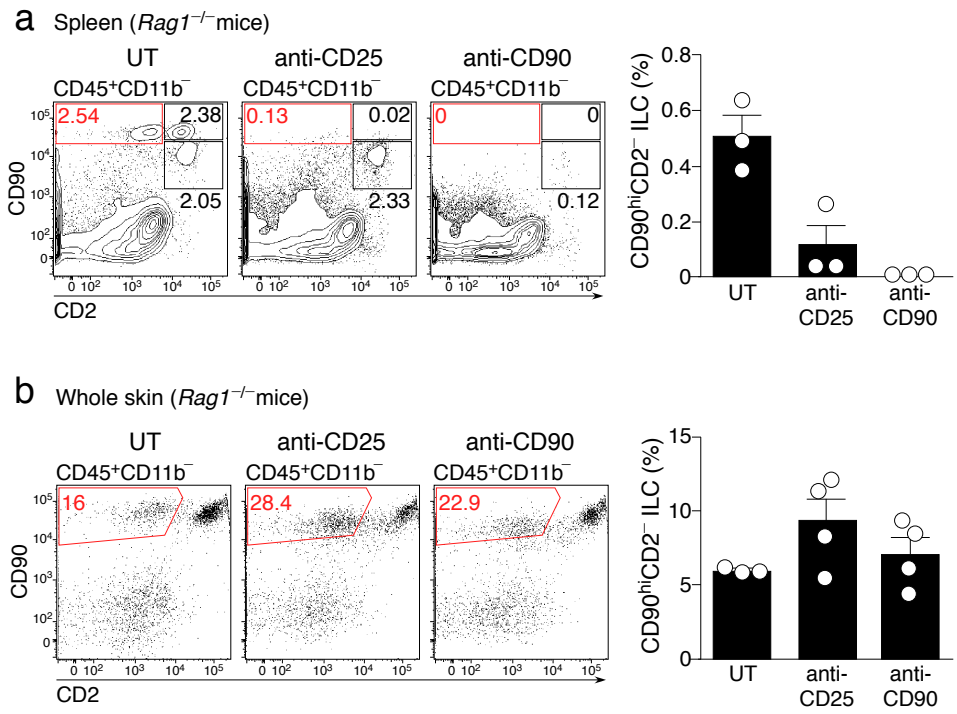

Supplementary Figure 6. ILC in the spleen and skin of mice treated with anti-CD25 and anti-CD90. (**a**) Left: Representative contour plots of $CD45^+CD11b^-$ splenocytes from untreated *Rag1*$^{-/-}$ mice and mice treated with either anti-CD25 (clone PC61) or anti-CD90.2 (clone 30H12). Mice were treated with 200 μg antibody per day for two days prior to assessment. CD90-expressing cells were detected using clone 53-2.1. Red boxes indicate $CD90^{hi}CD2^-$ ILC. Right: percentage of $CD90^{hi}CD2^-$ ILC (of total $CD45^+$ cells) in the spleens of antibody-treated mice. (**b**) Left: Representative contour plots of $CD45^+CD11b^-$ skin cells from untreated *Rag1*$^{-/-}$ mice and mice treated with either anti-CD25 or anti-CD90 as described in (a). Red boxes indicate $CD90^{hi}CD2^-$ dILC2. Right: Percentage of $CD90^{hi}CD2^-$ dILC2 (of total $CD45^+$ cells) in the skin of antibody-treated mice. Data in (a) and (b) are mean ± s.e.m. from 2 independent experiments. Symbols represent individual mice.

Supplementary Figure 7

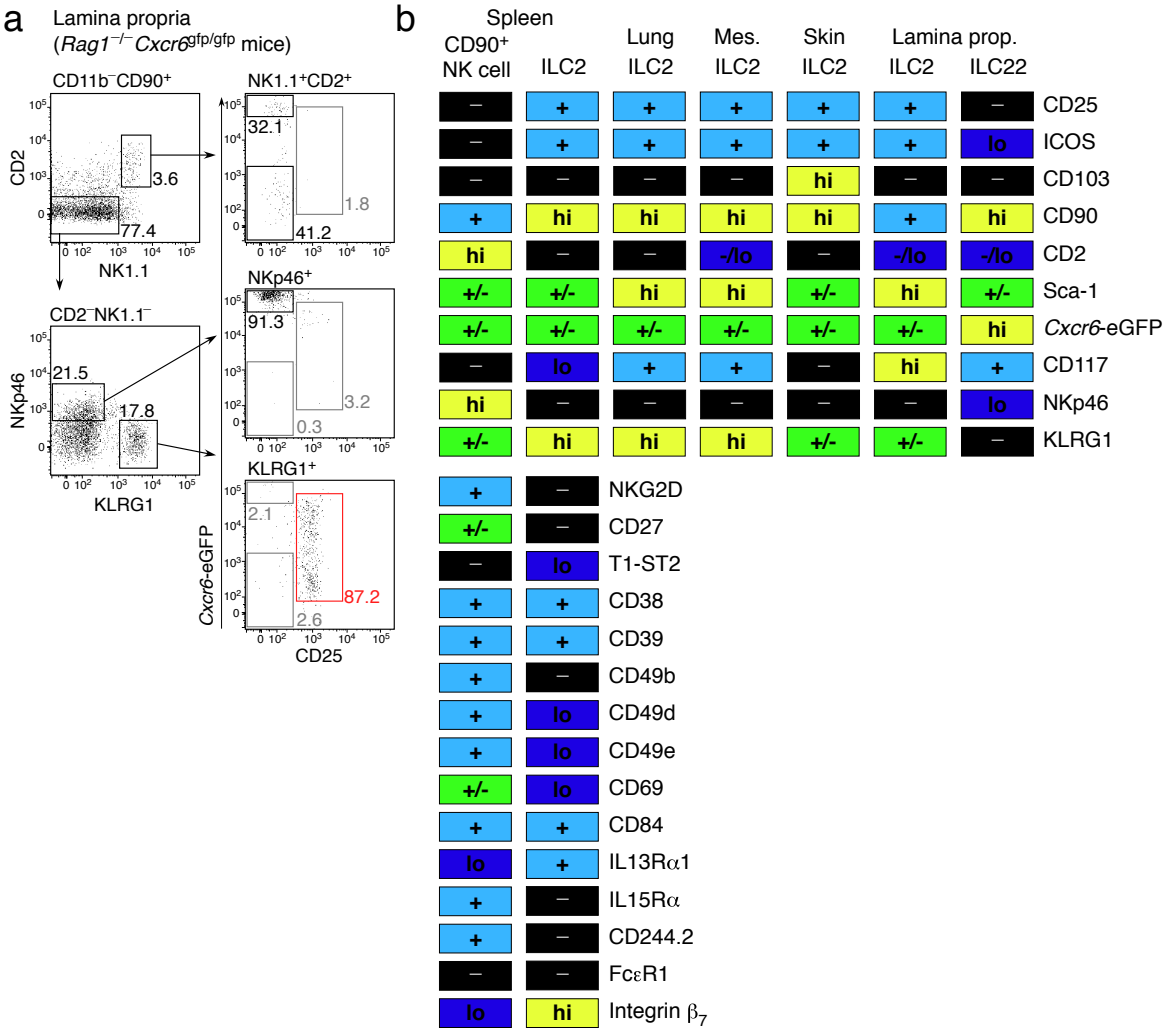

Supplementary Figure 7. Comparative phenotype of NK cells, NKp46^{+} ILC and ILC2 in *Rag1*$^{-/-}$ mice. (**a**) Representative dotplots depicting *Cxcr6*-eGFP and CD25 expression by NK1.1^{+} NK cells, NKp46^{+} ILC22 and KLRG1^{+} ILC2 (ref. 38) isolated from the lamina propria of *Rag1*$^{-/-}$ *Cxcr6*$^{+/gfp}$ mice. Data are representative of two independent experiments ($n = 2$). (**b**) Summary of cell surface expression (flow cytometry) of indicated proteins by NK cells, NKp46^{+} ILC and ILC2 from spleen, lung, mesentery, skin and lamina propria of *Rag1*$^{-/-}$ mice. −, not detected; +, positive; hi, high expression; lo, low expression; +/−, expression by some but not all cells. Data are summarized from 3 independent experiments ($n \geq 2$ per marker).

Supplementary Figure 8

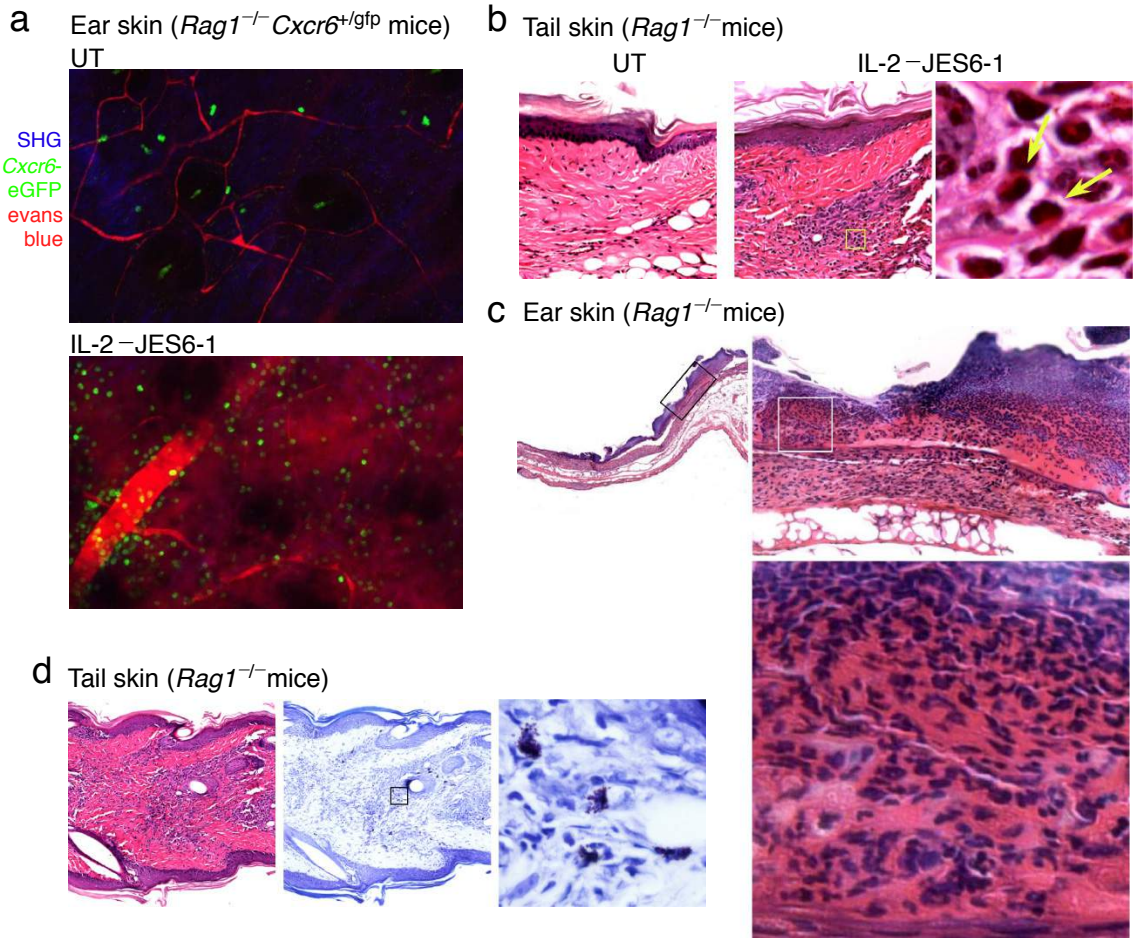

Supplementary Figure 8. IL-2-induced skin inflammation. (**a**) Representative images of IL-2–JES6-1 treated and untreated *Rag1*$^{-/-}$ *Cxcr6*$^{+/gfp}$ mouse skin by intravital multiphoton microscopy. Each image is a *z*-projection through a volume of 88 μm within the dermis, obtained 30 min after injection of Evans blue (red). Extracellular matrix in the dermis was detected by SHG signals (blue). dILC2 shown in green. (**b**) Tail sections obtained from untreated and IL-2-treated *Rag1*$^{-/-}$ mice, stained with hematoxylin and eosin. Yellow arrows indicate eosinophils. (**c**) Ear section obtained from an IL-2-treated *Rag1*$^{-/-}$ mouse, cut through a spontaneous lesion. Enlarged regions indicated the thickened epidermis with attached crusts and leukocyte infiltrate. (**d**) Tail sections obtained from an IL-2-treated *Rag1*$^{-/-}$ mouse, stained with hematoxylin and eosin (left) or toluidine blue (middle and right). Enlarged region indicates rounded, hypodense mast cells. Data in (a), (b), (c) and (d) are representative of two independent experiments ($n = 4$).